



PI-RADS 2.1: A Practical Overview

A. Dayala Sundaram¹

¹ Department of Radiology, Apollo Hospitals, Chennai, Tamil Nadu, India

J Gastrointestinal Abdominal Radiol ISGAR

Address for correspondence A. Dayala Sundaram, MBBS, DMRD, DNB, EdIR, Fellow in Onco-Imaging, Department of Radiology, Apollo Hospitals, 5/3, Masi Illam, D'Silva Road, Mylapore, Chennai, Tamil Nadu 600004, India (e-mail: dayalasundaram@gmail.com).

Abstract

The Prostate Imaging Reporting and Data System (PI-RADS) is an essential tool for standardizing the interpretation of multiparametric magnetic resonance imaging (mp-MRI) of the prostate for detecting prostate cancer. This article provides a comprehensive overview of the latest version, PI-RADS 2.1, with clear pictures to guide radiologists in its practical application for improved diagnostic accuracy. The article explores the key modifications, emphasizing the changes in scoring criteria and their impact on clinical decision-making. It discusses the importance of mp-MRI sequences, such as T2-weighted imaging, diffusion-weighted imaging, and dynamic contrast-enhanced imaging, and clarifies their significance in the PI-RADS 2.1 framework. The article highlights practical insights to help radiologists integrate this updated system into their day-to-day practice, promoting consistency and reliability in reporting.

Keywords

- ▶ overview
- ▶ PI-RADS 2.1
- ▶ practical

Introduction

Prostate cancer is a globally prevalent solid organ malignancy and ranks as the second most common cancer in men.¹⁻³ In India, it accounts for 9% of cancer-related mortality.⁴ Traditional screening methods for prostate cancer detection include serum prostate-specific antigen (PSA) evaluation and digital rectal examination. Systematic transrectal ultrasound-guided biopsies are done for pathological evaluation of abnormal findings. However, a combination of these screening methods carries the risk of both overdiagnosis of indolent tumors and underdiagnosis of clinically significant prostate cancer (csPCa; Gleason score of ≥ 7 [including International Society of Urological Pathology 2–Gleason score 3 + 4, with prominent but not predominant Gleason 4 component], a tumor volume of ≥ 0.5 mL, or the presence of extraprostatic extension [EPE]).⁵⁻⁸ The advent of multiparametric magnetic resonance imaging (mp-MRI) has brought about a paradigm shift in prostate cancer detection, offering a well-balanced approach to avoid both underdiagnosis and overtreatment. mp-MRI combines morphological assessment using T1 (T1WI)- and T2-weighted imaging (T2WI) with molecular and physiological evaluation through

diffusion-weighted imaging (DWI) and dynamic contrast-enhanced (DCE) imaging. mp-MRI has significantly increased sensitivity and negative predictive value in diagnosing csPCa.⁹⁻¹¹ To standardize the image acquisition, interpretation, and reporting of mp-MRI, Prostate Imaging Reporting and Data System (PI-RADS) was introduced in 2012. PI-RADS versions 2 and 2.1 were released later (2015 and 2019, respectively) with various revisions.⁷

MRI Sequences (PI-RADS 2.1)⁷

Though prostate MRI can be performed at both 1.5T and 3T, as per PI-RADS 2.1, 3T is preferred for the prostate MRI. At 3T, without use of an endorectal coil (ERC), image quality can be comparable with that obtained at 1.5 T with an ERC. Though ERC is considered indispensable for high-resolution diagnostic quality images in older 1.5T MRI systems, satisfactory results have been obtained at both 1.5T and 3T without the use of an ERC. Hence, use of ERC is optional for prostate MRI.

As MRI interpretation may be affected by postbiopsy changes such as hemorrhage and inflammation, an interval of at least 6 weeks or longer between biopsy and MRI should be considered.

DOI <https://doi.org/10.1055/s-0044-1787295>.
ISSN 2581-9933.

© 2024. The Author(s).

This is an open access article published by Thieme under the terms of the Creative Commons Attribution License, permitting unrestricted use, distribution, and reproduction so long as the original work is properly cited. (<https://creativecommons.org/licenses/by/4.0/>)
Thieme Medical and Scientific Publishers Pvt. Ltd., A-12, 2nd Floor, Sector 2, Noida-201301 UP, India

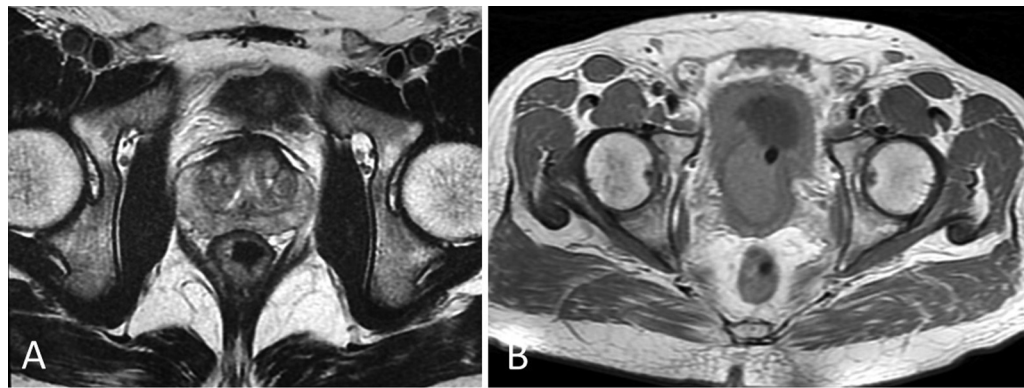


Fig. 1 Anatomic coverage for multiparametric magnetic resonance imaging (mp-MRI). Small field of view (FOV) for axial T2-weighted image (T2WI) (A) and large FOV for axial T1WI (B).

The recommended sequences are:

1. High-resolution T2WI (axial plane and a minimum of one additional orthogonal plane)
2. Axial DWI with apparent diffusion coefficient (ADC) map
3. Axial T1WI
4. Axial DCE imaging

MR spectroscopy was recommended in PI-RADS v1. However, its routine clinical application did not demonstrate any added value despite extending the study duration and necessitating dedicated software. Hence, MR spectroscopy was excluded from PI-RADS v2.

When prostate MRI is performed without DCE, it is termed as “biparametric MRI (bp-MRI).” Though transition zone (TZ) assessment remains unchanged when DCE is not performed, in some cases, DCE can aid in detection of csPCa in both peripheral zone (PZ) and TZ especially when T2/DWI sequences are suboptimal. So PI-RADS 2.1 favors mp-MRI over bp-MRI and bp-MRI should only be reserved for select clinical situations.

The anatomic coverage for high-resolution T2WI is as follows. Craniocaudally, from the neck of the bladder (including the entire seminal vesicles) to the prostate apex. Anteroposteriorly, the coverage extends from the pubic symphysis and includes the rectum. Laterally, the medial aspect of both femoral heads should be included. For T1WI, a large field of view is employed, extending from the aortic bifurcation to the pubic symphysis to evaluate the pelvic lymph nodes and bones (►Fig. 1). Further, T1 images are useful for identification of hemorrhage within prostate and seminal vesicles.

To facilitate synchronized scrolling and effective correlation, the imaging plane angle, location, and slice thickness must remain consistent across T2W, DWI, and DCE sequences (►Table 1).

Patient Preparation

1. Fasting is not mandatory as it does not substantially decrease bowel movement or rectal air.

Table 1 Recommended sequences for mp-MRI for prostate

Sequences	Plane	Technical specifications
High-resolution T2WI	Axial and sagittal/coronal	(1) Slice thickness: 3 mm, no gap. Imaging planes should be the same as those used for DWI and DCE (2) FOV: generally 12–20 cm to encompass the entire prostate gland and seminal vesicles (3) In plane dimension: ≤ 0.7 mm (phase) $\times \leq 0.4$ mm (frequency)
DWI with ADC map	Axial	(1) Slice thickness: ≤ 4 mm, no gap. Imaging planes should match or be similar to those used for T2W and DCE (2) FOV: 16–22 cm (3) In plane dimension: ≤ 2.5 mm both phase and frequency (4) <i>b</i> -value of at least 1400 sec/mm ²
T1WI	Axial	(1) Wider field of view to evaluate pelvic lymph nodes and bones
DCE	Axial	(1) 3D T1W GRE is preferred (2) Slice thickness: 3 mm, no gap. Imaging planes should be the same as those used for DWI and DCE (3) FOV: encompass the entire prostate gland and seminal vesicles (4) In plane dimension: ≤ 2 mm $\times \leq 2$ mm (5) Temporal resolution: ≤ 15 s (6) Total observation rate: > 2 min

Abbreviations: 3D, three-dimensional; ADC, apparent diffusion coefficient; DCE, dynamic contrast enhancement; DWI, diffusion-weighted imaging; FOV, field of view; GRE, gradient echo; mp-MRI, multiparametric magnetic resonance imaging; T1WI, T1-weighted imaging; T2WI, T2-weighted imaging.

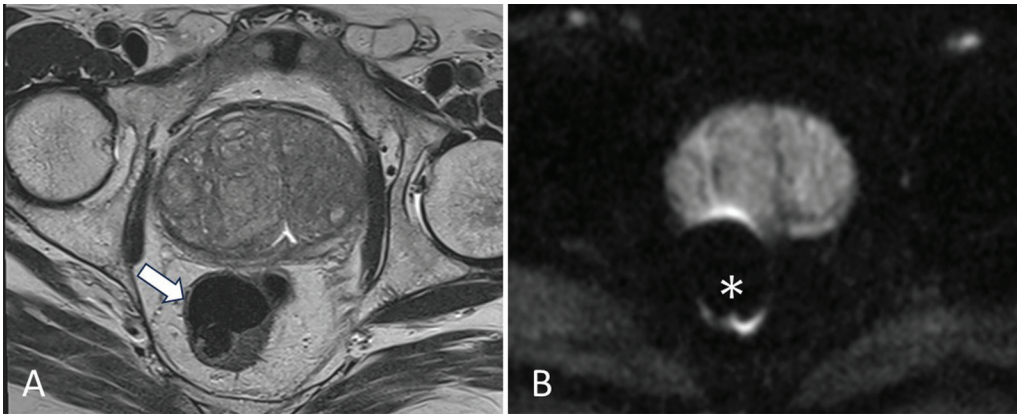


Fig. 2 Impact of rectal air. Air pocket (arrow) in the rectum on axial T2-weighted image (T2WI) (A) causing focal distortion on axial diffusion-weighted imaging (DWI) (asterisk) (B).

2. Antispasmodic agent is generally not required. Its usage may improve the quality of T2W images by reducing peristalsis-related motion artifacts. However, it does not substantially improve DWI quality.¹²
3. Enema is not routinely advocated. In cases where there is the presence of air or stool in the rectum, it may impact the quality of DWI (→**Fig. 2**). Therefore, if possible, it is recommended that the patient be encouraged to empty the rectum just before the MRI examination.
4. Some studies have proposed abstaining from ejaculation for 3 days prior to the MRI examination to achieve adequate distension of seminal vesicles since a significant decrease in seminal vesicle volume following ejaculation may compromise the assessment of potential seminal vesicle invasion in patients with known prostate cancer.¹³⁻¹⁵ However, this is not a routine requirement in day-to-day radiology practice.

Normal MR Anatomy of the Prostate

Lobar anatomy model was followed in the 19th and early 20th centuries. However, John E. McNeal (1930–2005), a clinical pathologist at Stanford University, presented his innovative perspective by categorizing prostate anatomy into four distinct anatomic zones,¹⁶ two glandular regions designated as the PZ and central zone (CZ), and an additional glandular region encompassing the prostatic urethra, known as the TZ and a nonglandular anterior fibromuscular stroma (AFMS).

PZ lies between the TZ and outer pseudocapsule, consisting of up to 70 to 80% of the glandular tissue. Approximately 70 to 75% of prostate cancers are found in the PZ. Due to high glandular content, the normal PZ usually appears homogeneously hyperintense on T2WI. Minimal background changes like scattered linear/wedge-shaped areas of intermediate signal intensity may be seen in some of the normal prostate glands¹⁷ (→**Fig. 3**). Altered T2 signal intensities are seen in the PZ in active prostatitis, postprostatitis sequelae, posthormonal, or chemotherapy and radiotherapy status. Due to high cellularity and less water content, the clinically significant cancer in the PZ appears as a hypointense focus.¹⁸

TZ lies between the urethra and outer PZ and extends inferiorly up to the verumontanum. It consists of only 5% of the glandular tissue and approximately 20 to 30% of prostate cancers occur in TZ. The TZ’s increased muscular components and dense stroma contribute to its relative T2 hypointensity compared to the PZ.¹⁹ In benign prostatic hyperplasia (BPH), the nodules in the transition may show myriad appearances. Predominantly glandular nodules may show moderate to marked T2 hyperintensity, predominantly stromal nodules show T2 hypointensity and mixed nodules may give an “organized chaos” pattern (→**Fig. 4**). Thus, the inherent heterogeneity in the TZ can pose significant challenges in detecting small T2 hypointense tumors.

CZ has an embryologically different origin, a Wolffian duct derivate. It surrounds the ejaculatory ducts and extends

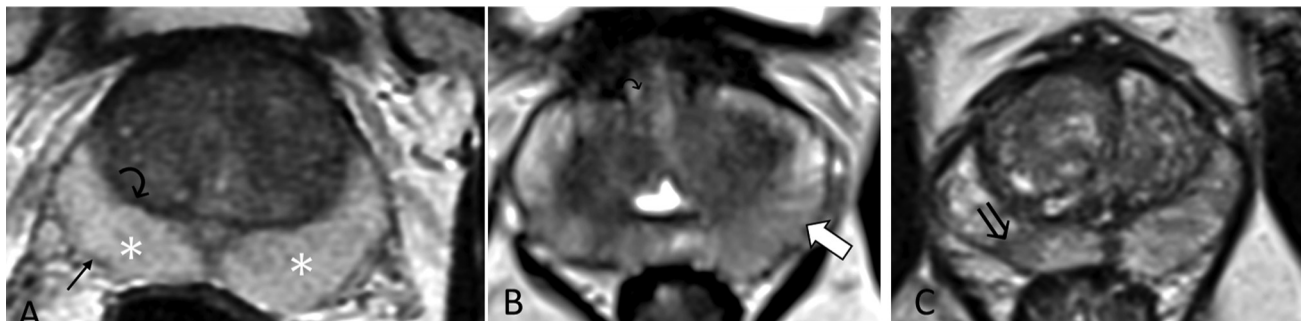


Fig. 3 T2 axial sections showing normal peripheral zone (A) between the surgical capsule (curved arrow) and outer pseudocapsule (straight arrow). Normal background variants with linear (B) and wedge-shaped (C) hypointensities.

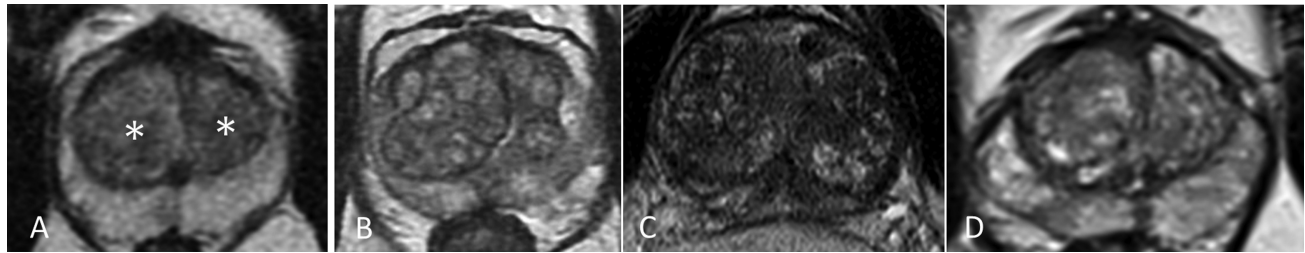


Fig. 4 T2 axial sections showing normal transition zone (TZ) (asterisks) (A). Various appearance of TZ in benign prostatic hyperplasia—predominantly glandular (B), stromal (C), and organized chaos (D) patterns.

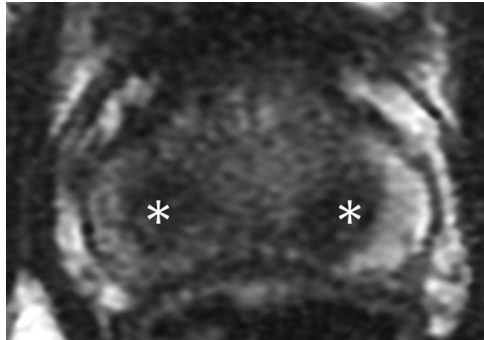


Fig. 5 T2 axial sections showing normal central zone (asterisks) seen as symmetric T2 hypointensity in the base.

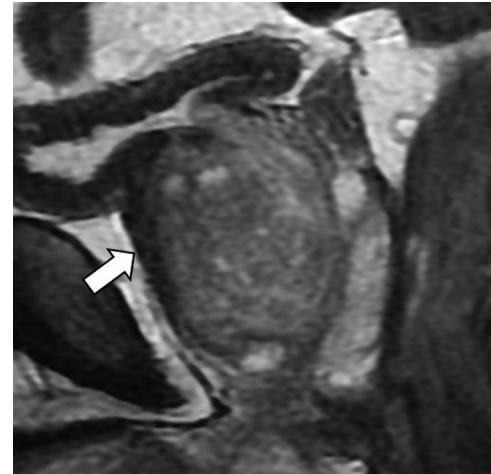


Fig. 6 Normal anterior fibromuscular stroma (arrow) seen as T2 linear T2 hypointensity in the sagittal plane.

inferiorly up to the level of verumontanum. It consists of about 20% of the glandular tissue. The stroma is densest in the CZ and typically shows a symmetric hypointensity in the base on T2WI²⁰ (→**Fig. 5**). Prostate cancer is relatively uncommon in this area and most of prostate cancers in CZ are extensions from PZ and TZ.⁷

AFMS, located anterior to the TZ, contains only fibromuscular tissue and lacks significant glandular tissue, hence appearing hypointense on T2WI. It is better appreciated on T2WI in the sagittal plane (→**Fig. 6**).

Seminal vesicles are seen in the superolateral aspect of the base of the prostate on both sides. On T2WI, due to the fluid content, normal seminal vesicles typically exhibit a

hyperintense signal similar to the appearance of a “cluster of grapes.” A mild degree of asymmetry is not uncommon (→**Fig. 7**).

Prostatic capsule, noted in the periphery of the gland, is not a true capsule, constituted by a band of concentrically arranged fibromuscular tissue indistinguishable from the prostatic stroma. It appears hypointense on T2WI. Another *pseudocapsule/surgical capsule* is noted at the interface of the TZ with the PZ (→**Fig. 8**). The surgical capsule is anchored

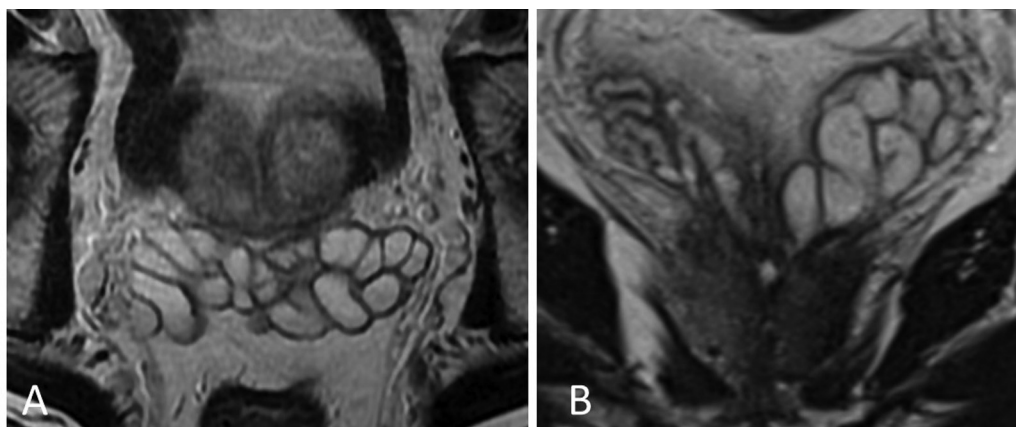


Fig. 7 Normal seminal vesicles showing “cluster of grapes” appearance on T2-weighted image (T2-weighted image (T2WI) axial plane (A). Normal variant with asymmetry in T2 coronal plane (B).

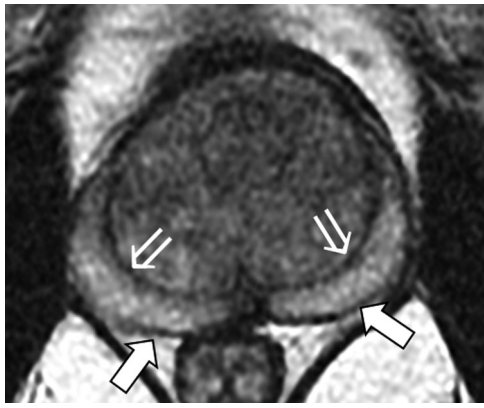


Fig. 8 T2 axial sections showing normal prostatic pseudocapsule in the periphery (white arrows) and surgical capsule (open arrows).

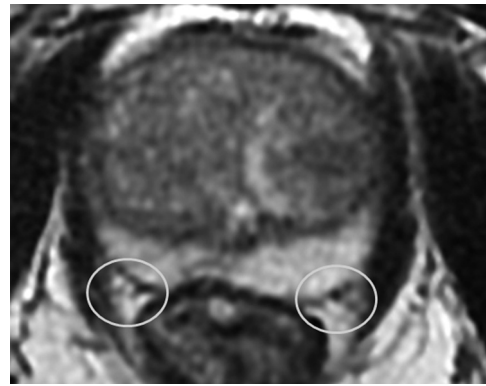


Fig. 10 Neurovascular bundles at 5 and 7 o'clock positions seen as small punctate dark structures in T2 axial sections.

superiorly to the smooth muscle of the base of the bladder. Hence, BPH nodule extends into the bladder along the plane of least resistance (►**Fig. 9**).²¹

Neurovascular bundles (NVBs) contain the arterial and venous prostatic vessels with cavernous nerves. The cavernous nerve contains sympathetic and parasympathetic fibers that supply the corpora cavernosa of the penis. On T2WI, they are noted at 5 and 7 o'clock positions as small punctate dark structures within the triangular fat signals (►**Fig. 10**).

Sectoral Map

The PI-RADS v2.1 segmentation model consists of 41 sectors/segments, including 38 for the prostate, 2 for the seminal vesicles, and 1 for the external urethral sphincter. Prostate is divided by an imaginary vertical line in the midline into the right and left lobes. Craniocaudally, it is divided into three equal regions: the base, mid gland, and apex. The PZ on both sides at each level has two sections: anterior (a) and posterior (p). The posterior segment is further divided into

medial posterior (mp) and lateral posterior (lp) segments. Similarly, the TZ on both sides at each level has two sections: anterior (a) and posterior (p) (►**Fig. 11**).

The sectoral map is a valuable tool for radiologists, urologists, and pathologists, enabling precise localization of findings mentioned in mp-MRI reports. It serves as a guide for MRI-targeted biopsies, therapies, and surgical procedures. Additionally, it can be employed as a visual aid during patient discussions about biopsy and treatment choices.

Lesion Assessment

Lesion assessment in the prostate can be simplified into three steps (►**Fig. 12**):

- Step 1: Localization of the lesion – identifying the anatomical location of the lesion, whether the lesion is situated in the PZ or TZ.
- Step 2: Primary scoring of the lesion based on dominant sequence: The dominant sequence for the lesion in the PZ is DWI, and for the TZ, it is T2WI.

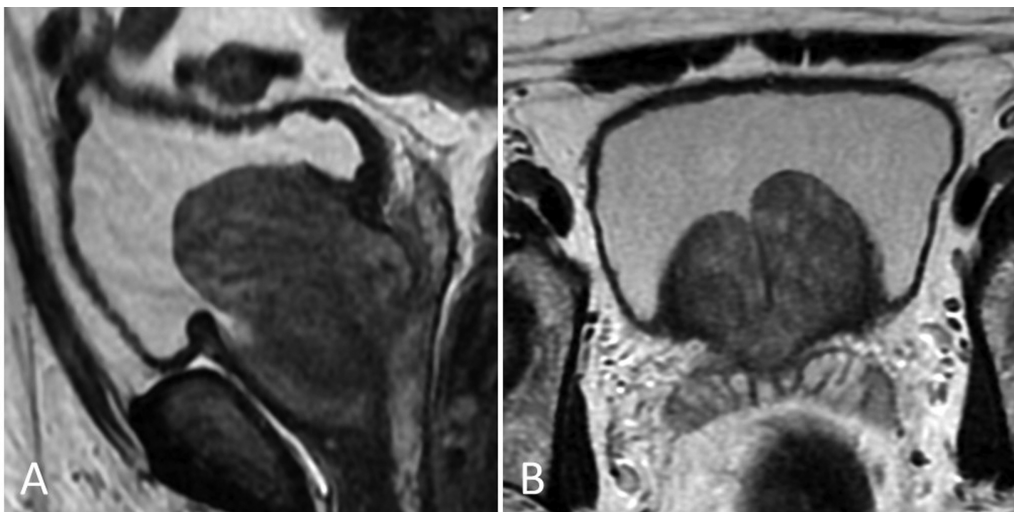


Fig. 9 Benign prostatic hypertrophy with enlarged transition zone extending into the bladder in sagittal (A) and axial (B) T2 sections.

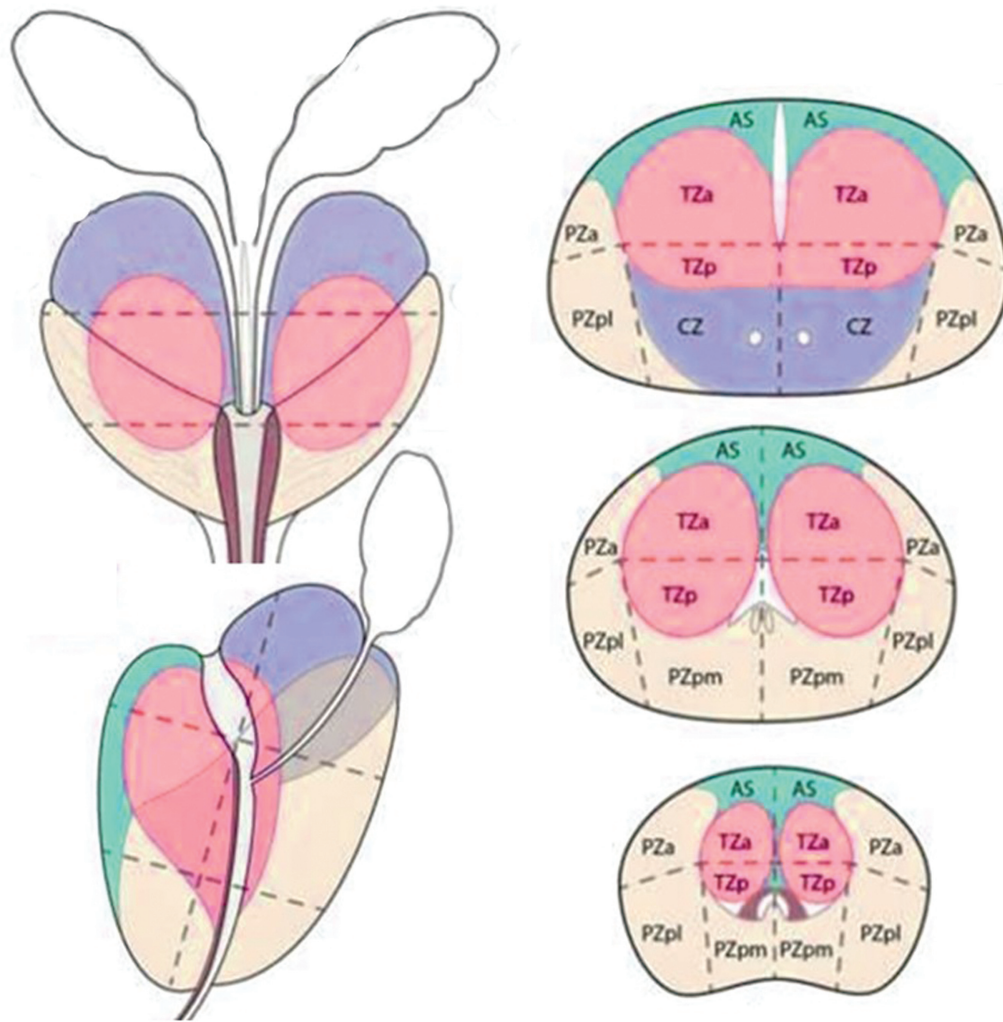


Fig. 11 Sectoral map.

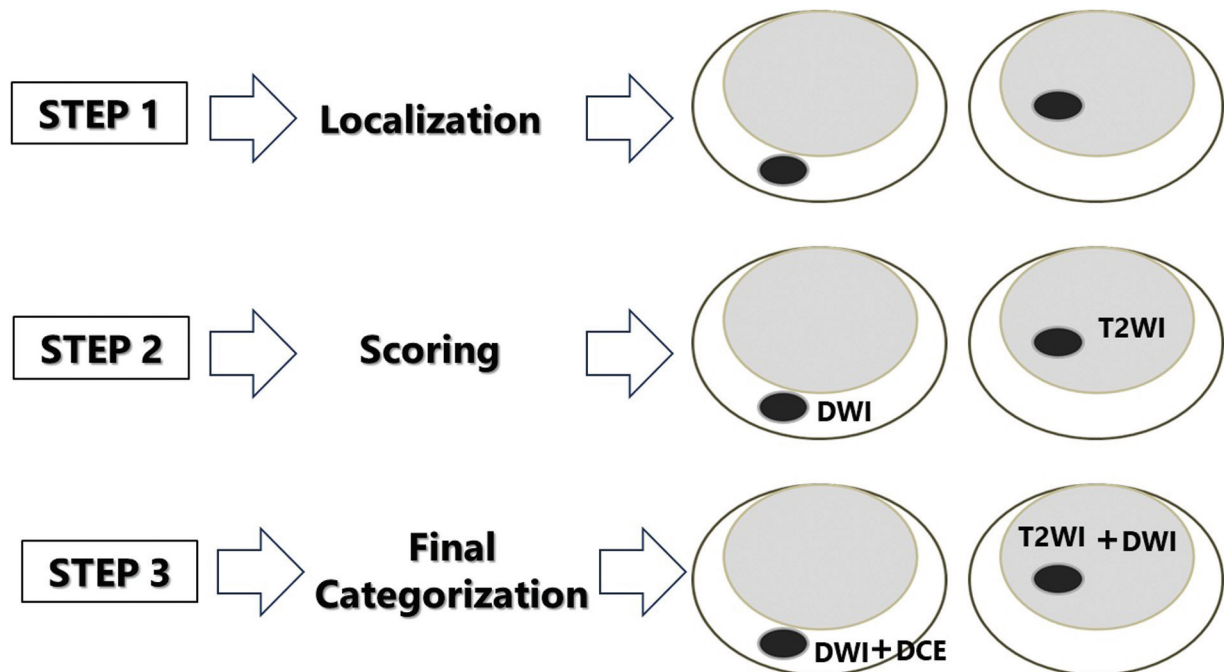


Fig. 12 Lesion assessment steps.

Step 3: Final categorization of the lesion based on the complementary sequences, that is, DCE for PZ lesion and DWI for TZ lesion.

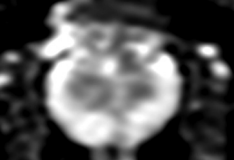

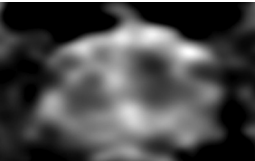
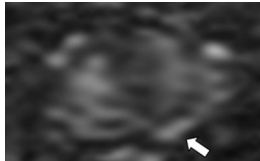
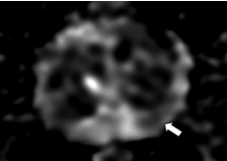
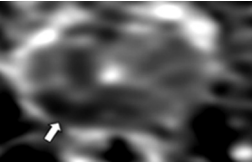
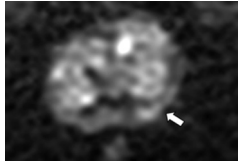
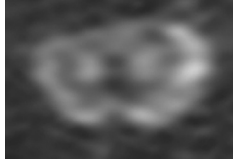
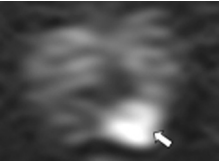
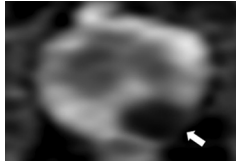
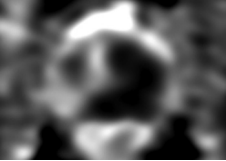

Peripheral Zone Lesion Assessment

Primary Scoring of PZ Lesion Based on DWI

Lesions in the PZ are assigned a score ranging from 1 to 5 based on the ADC map in conjunction with the corresponding DWI (► **Table 2**).

“Marked hyperintensity” on DWI is defined as a more pronounced signal change than any other focus in the same zone. When reviewing ADC maps, it is essential to use standard grayscale mode. A fixed “prostate window” is not universally applicable across all MRI scanners. It is essential to determine the appropriate window width and level (e.g., 1400:1400) tailored to each scanner, ensuring that csPCa appears markedly hypointense on the ADC map. Consistency in applying these settings across all mp-MRI studies is crucial.

Table 2 Primary scoring of PZ lesion based on DWI

ADC map	DW image	Score
		1
No abnormality on ADC and high <i>b</i> -value DWI (i.e., normal)		
		2
Linear or wedge-shaped hypointensity on ADC and/or linear wedge-shaped hyperintensity on high <i>b</i> -value DWI		
 	 	3
Focal hypointensity (discrete and different from the background) on ADC and/or focal hyperintensity on high <i>b</i> -value DWI		
		5
Focal marked hypointensity on ADC map and marked hyperintensity on high <i>b</i> -value DWI; < 1.5 cm in greatest dimension		
		5
Same as 4 but size of the lesion ≥ 1.5 cm in greatest dimension/definite extraprostatic extension/invasive behavior		

Abbreviations: ADC, apparent diffusion coefficient; DWI, diffusion-weighted imaging; PZ, peripheral zone.

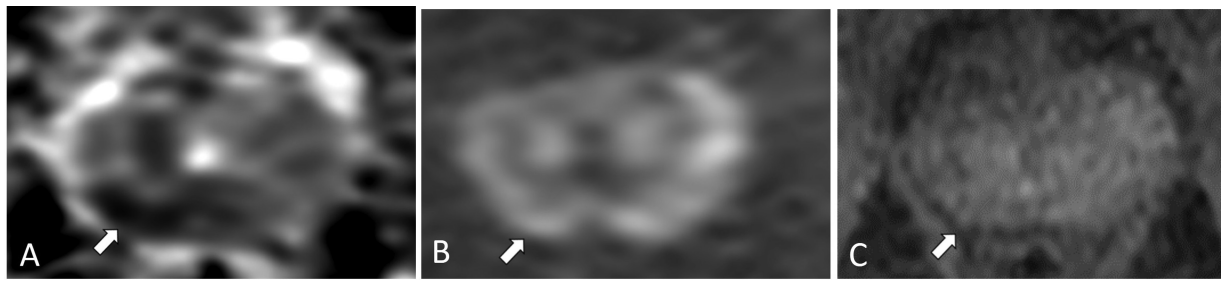


Fig. 13 Prostate Imaging Reporting and Data System (PI-RADS) score 3 lesion (A, B – apparent diffusion coefficient [ADC]/diffusion-weighted imaging (diffusion-weighted imaging [DWI] axial sections) with no significant early enhancement (C – dynamic contrast-enhanced [DCE] T1 axial sections), remains as PI-RADS 3 final category.

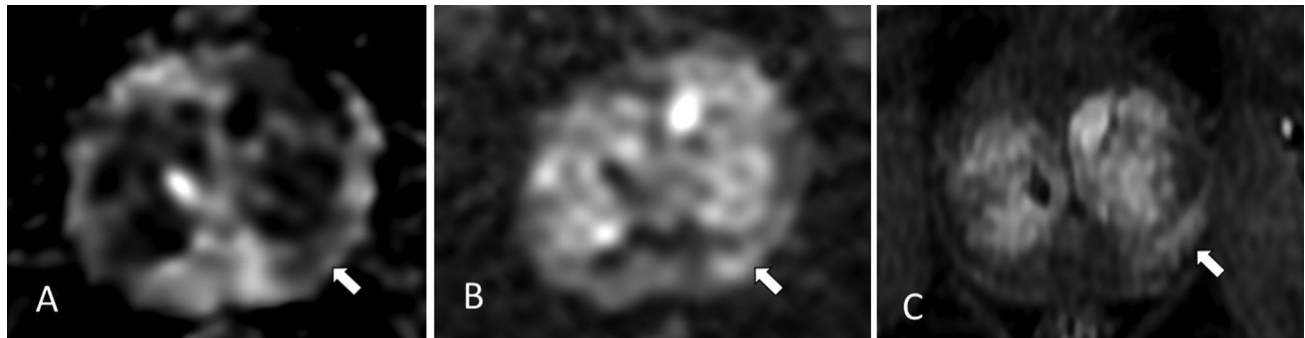


Fig. 14 Prostate Imaging Reporting and Data System (PI-RADS) score 3 lesion (A, B – apparent diffusion coefficient [ADC]/diffusion-weighted imaging [DWI] axial sections) with early enhancement (C – dynamic contrast-enhanced [DCE] T1 axial sections), can be upgraded to PI-RADS 4 final category.

Final Categorization of PZ Lesion

Lesions with DWI scores of 1, 2, 4, and 5 can be directly equated to final PI-RADS categories of 1, 2, 4, and 5, respectively. However, further evaluation is recommended

for a lesion with a DWI score of 3, using DCE. If the lesion reveals early enhancement, it can be upgraded to PI-RADS category 4 and the lesion without significant early enhancement, remains in category PI-RADS 3 (>Figs. 13 and 14).

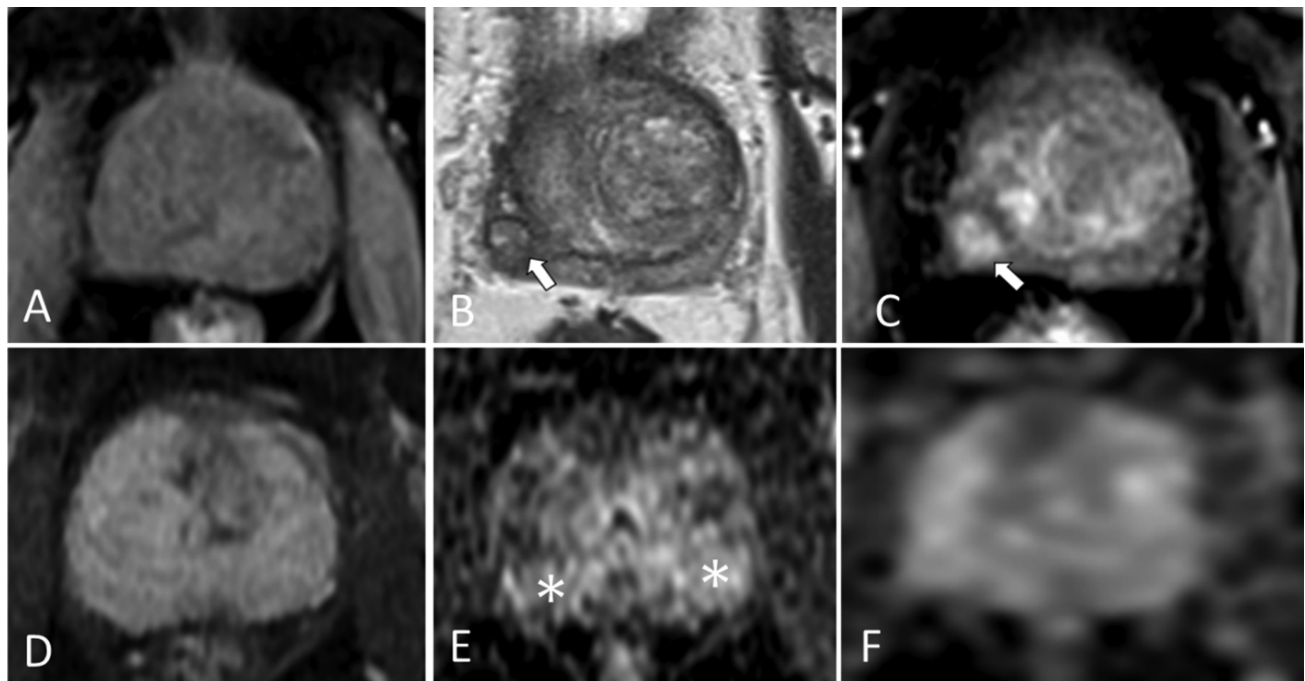


Fig. 15 Dynamic contrast-enhanced (DCE) negative categories. Absent early enhancement (A – DCE T1 axial), early enhancement in the extruded nodule (arrows) (B – T2 axial, C – diffusion-weighted imaging [DWI] axial), widespread enhancement (D – DCE T1 axial), enhancement without corresponding restricted diffusion (E – apparent diffusion coefficient [ADC] axial, F – DWI axial).

DCE positivity is indicated by focal enhancement that occurs earlier than the surrounding normal prostatic tissue, correlating with suspicious findings observed in T2WI and/or DWI. On the other hand, the following scenarios are considered DCE negative:

- Absence of early enhancement
- Focal enhancement that corresponds to a benign hyperplastic nodule on T2WI, including extruded benign hyperplastic nodules in the PZ
- Multifocal or widespread enhancement that does not correlate with focal findings on T2WI and/or DWI (► Fig. 15)

further evaluation using DWI is recommended for a lesion with a T2WI score of 2 and 3. For lesions in the TZ initially rated as PI-RADS score 2, if they show significant restricted diffusion (with a DWI score of 4 or higher), their overall PI-RADS classification can be raised to category 3 (► Fig. 16). Similarly, lesions initially assigned a PI-RADS score of 3 may be upgraded to category 4 if they present with a DWI score of 5 (► Fig. 17).

Overall PI-RADS Category

Peripheral Zone		Overall Assessment Category	Transition Zone	
DWI				T2WI
Score 1	→	PI-RADS 1	←	Score 1
Score 2	→	PI-RADS 2	←	Score 2
Score 3	→ DCE - → DCE +	PI-RADS 3	← DWI ≥ 4 ← DWI 5	Score 3
Score 4	→	PI-RADS 4	←	Score 4
Score 5	→	PI-RADS 5	←	Score 5

Transition Zone Lesion Assessment

Primary Scoring of TZ Lesions Based on T2WI

Lesions in the TZ are assigned a score ranging from 1 to 5 based on the T2WI characteristics. The evaluation predominantly relies on the T2 hypointensity, shape, and margins of the lesions (► Table 3).

Classic encapsulated BPH nodules are given a PI-RADS score of 1. Even BPH nodules that show marked restricted diffusion due to high cellularity can still be categorized as score 1. Atypical nodules, particularly those that are not fully encapsulated and the hypointense areas between nodules, are classified under score 2.

Final Categorization of TZ Lesion

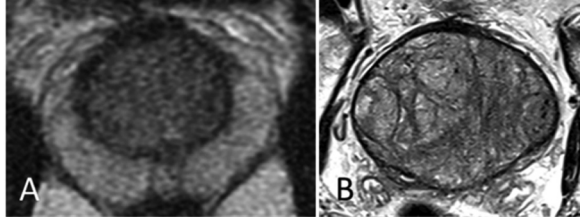
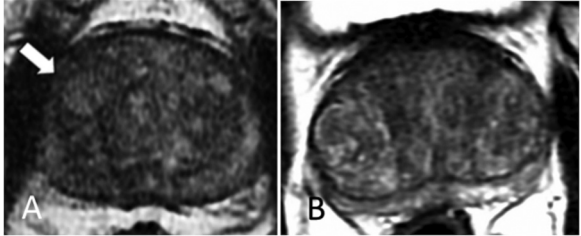

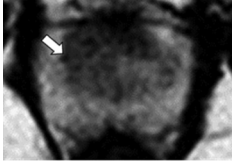
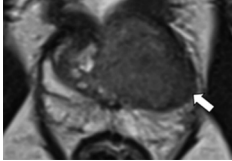
Lesions with T2WI scores of 1, 4, and 5 can be directly equated to final PI-RADS categories of 1, 4, and 5, respectively. However,

Evaluation of Central Zone

The normal CZ typically appears as symmetric low T2 signal intensity at the base of the prostate and can be identified in up to 93% of MRI cases.^{20,22} In cases of benign prostatic hypertrophy, the CZ may be compressed by benign prostatic hyperplastic nodules against the TZ, leading to distinctive signs. The “mustache” sign refers to the compressed CZ appearing as symmetric, bilateral areas of low signal intensity on T2WI at the base/middle of the prostate, flanking the ejaculatory ducts. The “teardrop” sign is characterized by the compressed CZ presenting as a median low signal intensity area at the middle third of the posterior aspect, extending up to the level of the verumontanum inferiorly²³ (► Fig. 18).

Although tumors originating from the CZ constitute less than 5% of all prostate cancers, they tend to be more aggressive, with a higher grade and an increased likelihood of extracapsular extension and seminal vesicle invasion.²⁴ Indicators of a tumor

Table 3 Primary scoring of TZ lesion based on T2WI

Description	T2WI image	Score
Normal appearing TZ (A) or typical nodule – round, completely encapsulated nodule (B)		1
Mostly encapsulated nodule or homogeneous circumscribed nodule without encapsulation - atypical nodule (A) Homogeneous mild mildly hypointense area between nodules (B)		2
Heterogeneous signal intensity with obscured margins. Includes others that do not qualify as to 4 or 5		3
Lenticular or noncircumscribed, homogeneous, moderately hypointense lesions measuring < 1.5 cm		4
Same as 4, but size of the lesion ≥ 1.5 cm/definite extraprostatic extension/invasive behavior		5

Abbreviations: T2WI, T2-weighted image; TZ, transition zone.

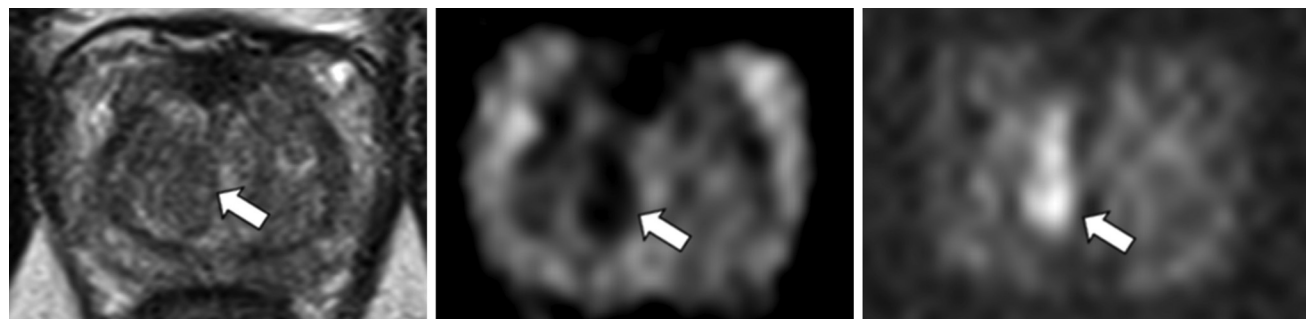


Fig. 16 T2 axial, apparent diffusion coefficient (ADC), and diffusion-weighted imaging (DWI) axial sections showing partially encapsulated nodule in the right transition zone with Prostate Imaging Reporting and Data System (PI-RADS) score 2 with DWI score 4, which can be upgraded to PI-RADS 3 final category.

in the CZ may include asymmetry in size, extension below the verumontanum, early enhancement, and restricted diffusion. Meanwhile, it is essential to note that in approximately 20% of cases, the CZ may exhibit asymmetry²⁵ (–Fig. 19).

Evaluation of Anterior Fibromuscular Stroma

The AFMS does not contain glandular tissue and is primarily composed of fibromuscular tissue. Due to its fibrous

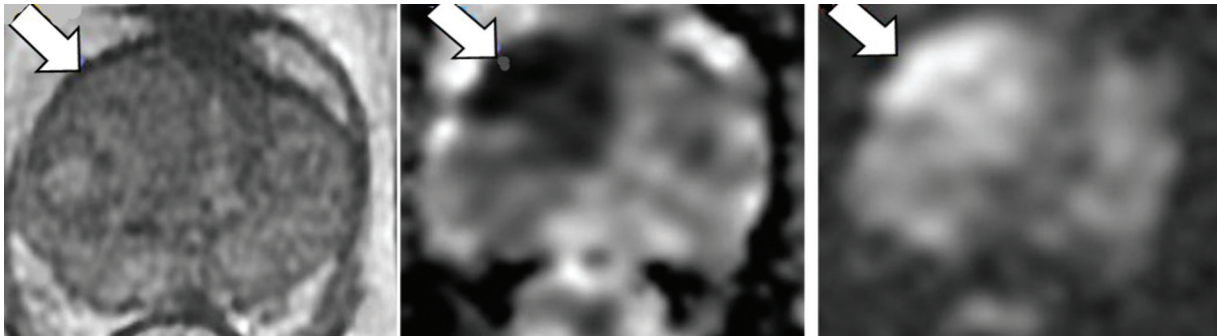


Fig. 17 T2 axial, apparent diffusion coefficient (ADC), and diffusion-weighted imaging (DWI) axial sections showing heterogeneous signal intensity with obscured margins in right transition zone with Prostate Imaging Reporting and Data System (PI-RADS) score 3 showing significant restricted diffusion, DWI score 5, which can be upgraded to PI-RADS 4 final category.

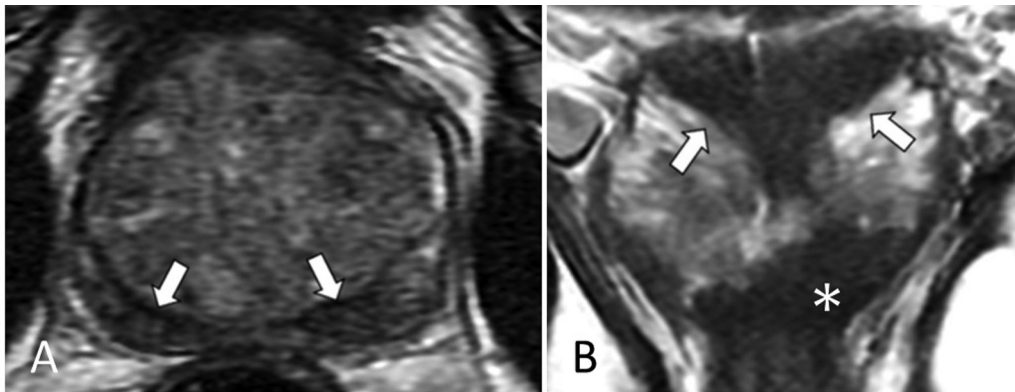


Fig. 18 “Mustache” sign (A – axial sections), the compressed central zone (CZ) appearing as symmetric, bilateral areas of low signal intensity on T2-weighted image (T2WI) at the base surrounding the ejaculatory ducts. “Teardrop” sign (B – coronal sections), the compressed CZ presenting as a median low signal intensity area at the middle third, extending up to the level of the verumontanum inferiorly. Carcinoma seen as ill-defined T2 hypointense lesion in the peripheral zone in the apex (asterisk).



Fig. 19 Asymmetric appearance of central zone in axial T2 sections.

composition, it usually shows low signal intensity on T2WI, ADC, and DWI, along with delayed enhancement. Due to absent glandular tissue, the possibility of cancer is practically not possible. However, tumors arising in the PZ or TZ can extend into the AFMS. For lesions involving the AFMS, the PI-RADS scoring is based on the characteristics of the zone from which the lesion appears to be originating (PZ or TZ) (► Fig. 20).

Extraprostatic Extension

EPE is characterized by capsule breach accompanied by clear signs of direct tumor spread, like the invasion of seminal vesicles, NVBs, or urinary bladder wall. Other indirect signs to be considered are loss of the rectoprostatic angle, asymmetry of the NVBs, the bulging contour of the prostate, and a tumor-capsule interface exceeding 1.0 cm^{26} (► Fig. 21).

Seminal Vesicle Invasion

Seminal vesicle invasion is characterized by evidence of direct tumor spread from the prostate base into and around the seminal vesicle, localized or widespread low T2W signal intensity, atypical contrast enhancement, and restricted diffusion within or surrounding the seminal vesicle. Another indicator is the obliteration of the angle between the prostate base and the seminal vesicle.²⁷ Seminal vesicle invasion may be of one of the three types: (1) tumor extension through the ejaculatory ducts, (2) direct spread from the prostatic base/extension into periprostatic fatty tissue and seminal vesicle invasion, and (3) tumor deposits (► Fig. 22). Seminal vesicle invasion is associated with an increased risk of lymph

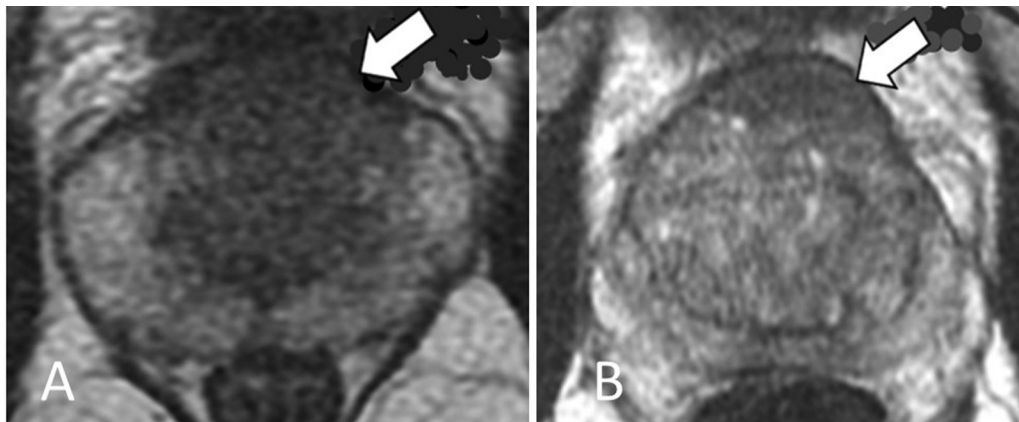


Fig. 20 T2 axial sections showing peripheral zone lesion involving the anterior fibromuscular stroma (AFMS) (A) and transition zone lesion involving the AFMS (B).

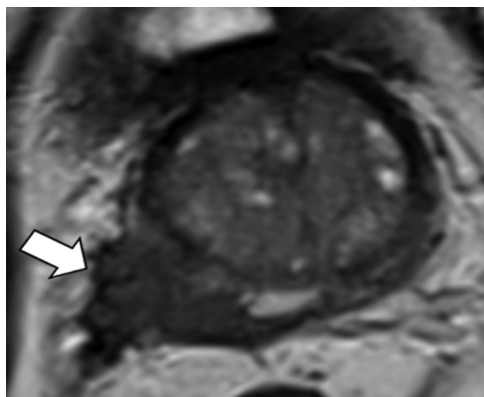


Fig. 21 T2 axial sections showing peripheral zone lesion with significant extraprostatic extension (arrow).

node or distant metastasis, early biochemical recurrence, and a poor prognosis.^{28–33}

Neurovascular Bundle Invasion

The NVBs lie in close proximity to the PZ, where the majority of cancer arises. NVB invasion is characterized by evidence of direct tumor spread from the prostate with obliteration of the fat signals at 5 or 7 o'clock positions

(► **Fig. 23**). Resection of the NVBs may lead to incontinence, impotence, and erectile dysfunction. Hence, various nerve-sparing surgical techniques are employed when the NVBs are unaffected.

Structured Reporting of mp-MRI

Prostate volume assessment is done with the ellipsoid formula (maximum anteroposterior × transverse × craniocaudal length × 0.52). The maximum craniocaudal and anteroposterior dimensions should be measured in the mid-sagittal image, while the transverse dimension should be measured in the axial dimension.

The derivatives of PSA are PSA density and PSA velocity. PSA density is calculated by dividing the PSA value by the prostate volume. It is a marker of aggressiveness of the tumor and PSA density of more than 0.15 correlates with high yield in biopsies. PSA velocity is the rate of PSA rise over a particular time period. PSA velocity of more than 0.75 ng/mL/y is significantly associated with prostate cancer. It is recommended to include PSA density in structured reporting of mp-MRI.^{34,35}

In lesion evaluation, it is advisable to begin with the corresponding dominant sequence for initial assessment and then the additional sequences for further characterization.

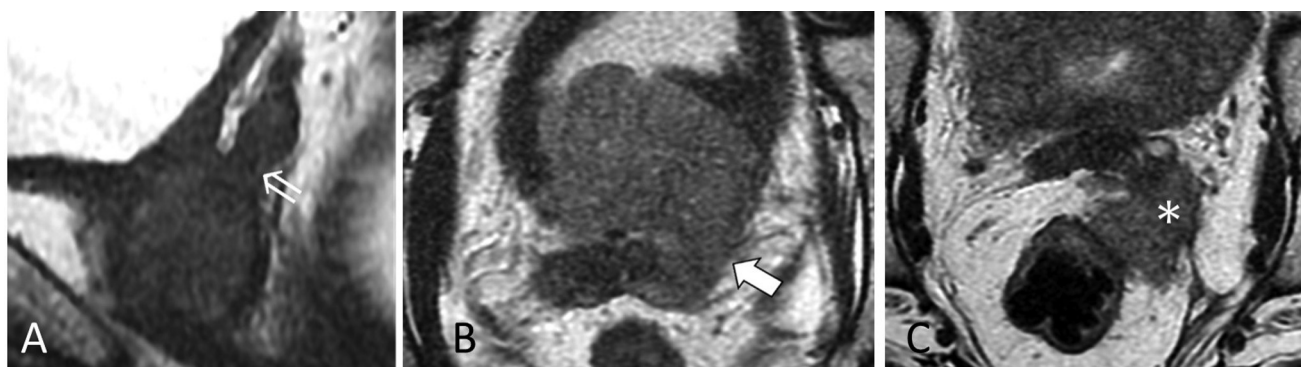


Fig. 22 Seminal vesicle extension—extension along the ejaculatory duct (open arrow) (A – T2 sagittal section), extension from the base of the prostate (arrow) (B – T2 axial section), and tumor deposit in the left seminal vesicle (asterisk) (C – T2 axial section).



Fig. 23 T2 axial sections showing neurovascular bundle invasion. (A) Bilateral neurovascular bundles are spared. (B) Unilateral involvement on the left side. (C) Bilateral involvement.

In cases where DWIs are significantly distorted due to metallic artifacts from hip prostheses, this should be clearly indicated in the report. Findings from T2WI and DCE should be relied upon to extract maximum diagnostic information.

Up to four lesions with PI-RADS assessment categories 3, 4, or 5 should be delineated on the sector map. The lesion with the highest PI-RADS category or one demonstrating EPE should be considered the index lesion. In instances where multiple lesions share the same highest category, the largest one should be designated as the index lesion.

While measuring the largest dimension of a lesion on an axial image is preferred, if the largest dimension is on sagittal or coronal images, the measurement and imaging plane should be clearly documented. For lesions in the PZ, measurements should be taken on ADC, while in the TZ, measurements should be based on T2WIs.

PI-RADS 2.1 recommends following reporting template:

Indication: (include the date and value of serum PSA level and any prior biopsy type, date, and results), prior therapy (radiation, hormones)

Technique: (state PI-RADS-compliance; explicit description of field strength, coils used, route and rate of intravenous contrast administration, and pulse sequence parameters is recommended)

Comparison: if present

Findings:

Size: L × W × H cm or V cubic cm (with inclusion of PSA density)

Quality

Hemorrhage:

PZ:

TZ:

Lesion (s) in rank order of severity (highest score to lowest score, then by size)

#1:

Location: use PI-RADS SECTOR LABEL and IMAGE SERIES/NUMBER

Size:

T2:

DWI:

DCE:

Prostate margin: (no involvement, indeterminate, or definite EPE)

Lesion overall PI-RADS category:

EPE:

NVBs: Distance from index lesion or any PI-RADS 4/5 lesion to NVB's

Seminal vesicles:

Lymph nodes

Other pelvic organs:

Impression:

Overall PI-RADS category (listing of PI-RADS categories)

Conclusion

In conclusion, this review accentuates the profound impact of PI-RADS 2.1 in prostate imaging. With a meticulous examination of imaging sequences and a systematic approach to lesion characterization, PI-RADS 2.1 emerges as a powerful and nuanced tool, significantly improving diagnostic accuracy for the benefit of both clinicians and patients. As technological advancements unfold, the continuous refinement of PI-RADS criteria assures its enduring relevance and efficacy. Its seamless integration into clinical practice hones risk stratification and serves as a guiding light for standardized reporting in prostate mp-MRI.

Conflict of Interest

None declared.

References

- 1 World Cancer Research Fund International/American Institute for Cancer Research Continuous Update Project Report. Diet, Nutrition, Physical Activity, and Prostate Cancer. 2014. Accessed May 16, 2024 at: www.wcrf.org/sites/default/files/Prostate-Cancer-2014-Report.pdf
- 2 Fitzmaurice C, et al. Global, regional, and national cancer incidence, mortality, years of life lost, years lived with disability, and disability-adjusted life-years for 32 cancer groups, 1990 to 2015. *JAMA Oncol* 2017;3:524
- 3 Siegel RL, Miller KD, Jemal A. Cancer statistics, 2018. *CA Cancer J Clin* 2018;68:7–30

- 4 Jemal A, Center MM, DeSantis C, Ward EM. Global patterns of cancer incidence and mortality rates and trends. *Cancer Epidemiol Biomarkers Prev* 2010;19(08):1893–1907
- 5 Schröder FH, Hugosson J, Roobol MJ, et al; ERSPC Investigators. Screening and prostate-cancer mortality in a randomized European study. *N Engl J Med* 2009;360(13):1320–1328
- 6 Loeb S, Bjurlin MA, Nicholson J, et al. Overdiagnosis and overtreatment of prostate cancer. *Eur Urol* 2014;65(06):1046–1055
- 7 Turkbey B, Rosenkrantz AB, Haider MA, et al. Prostate Imaging Reporting and Data System Version 2.1: 2019 Update of Prostate Imaging Reporting and Data System Version 2. *Eur Urol* 2019;76(03):340–351
- 8 Arif M, Schoots IG, Castillo Tovar J, et al. Clinically significant prostate cancer detection and segmentation in low-risk patients using a convolutional neural network on multi-parametric MRI. *Eur Radiol* 2020;30(12):6582–6592
- 9 Padhani AR, Weinreb J, Rosenkrantz AB, Villeirs G, Turkbey B, Barentsz J. Prostate imaging reporting and data system steering committee: PI-RADS v2 status update and future directions. *Eur Urol* 2019;75(03):385–396
- 10 Moldovan PC, Van den Broeck T, Sylvester R, et al. What is the negative predictive value of multiparametric magnetic resonance imaging in excluding prostate cancer at biopsy? A systematic review and meta-analysis from the European association of urology prostate cancer guidelines panel. *Eur Urol* 2017;72(02):250–266
- 11 Woo S, Suh CH, Kim SY, Cho JY, Kim SH. Diagnostic performance of Prostate Imaging Reporting and Data System version 2 for detection of prostate cancer: a systematic review and diagnostic meta-analysis. *Eur Urol* 2017;72(02):177–188
- 12 Slough RA, Caglic I, Hansen NL, Patterson AJ, Barrett T. Effect of hyoscine butylbromide on prostate multiparametric MRI anatomical and functional image quality. *Clin Radiol* 2018;73(02):216.e9–216.e14
- 13 Kabakus IM, Borofsky S, Mertan FV, et al. Does abstinence from ejaculation before prostate MRI improve evaluation of the seminal vesicles? *AJR Am J Roentgenol* 2016;207(06):1205–1209
- 14 Barrett T, Tanner J, Gill AB, Slough RA, Wason J, Gallagher FA. The longitudinal effect of ejaculation on seminal vesicle fluid volume and whole-prostate ADC as measured on prostate MRI. *Eur Radiol* 2017;27(12):5236–5243
- 15 Shin T, Kaji Y, Shukuya T, Nozaki M, Soh S, Okada H. Significant changes of T2 value in the peripheral zone and seminal vesicles after ejaculation. *Eur Radiol* 2018;28(03):1009–1015
- 16 Selman SH. The McNeal prostate: a review. *Urology* 2011;78(06):1224–1228
- 17 Bura V, Caglic I, Snoj Z, et al. MRI features of the normal prostatic peripheral zone: the relationship between age and signal heterogeneity on T2WI, DWI, and DCE sequences. *Eur Radiol* 2021;31(07):4908–4917
- 18 Barentsz JO, Richenberg J, Clements R, et al; European Society of Urogenital Radiology. ESUR prostate MR guidelines 2012. *Eur Radiol* 2012;22(04):746–757
- 19 Kayhan A, Fan X, Oommen J, Oto A. Multi-parametric MR imaging of transition zone prostate cancer: imaging features, detection and staging. *World J Radiol* 2010;2(05):180–187
- 20 Vargas HA, Akin O, Franiel T, et al. Normal central zone of the prostate and central zone involvement by prostate cancer: clinical and MR imaging implications. *Radiology* 2012;262(03):894–902
- 21 Rosenkrantz AB, Taneja SS. Radiologist, be aware: ten pitfalls that confound the interpretation of multiparametric prostate MRI. *AJR Am J Roentgenol* 2014;202(01):109–120
- 22 Hansford BG, Karademir I, Peng Y, et al. Dynamic contrast-enhanced MR imaging features of the normal central zone of the prostate. *Acad Radiol* 2014;21(05):569–577
- 23 Panebianco V, Giganti F, Kitzing YX, et al. An update of pitfalls in prostate mpMRI: a practical approach through the lens of PI-RADS v. 2 guidelines. *Insights Imaging* 2018;9(01):87–101
- 24 Cohen RJ, Shannon BA, Phillips M, Moorin RE, Wheeler TM, Garrett KL. Central zone carcinoma of the prostate gland: a distinct tumor type with poor prognostic features. *J Urol* 2008;179(05):1762–1767, discussion 1767
- 25 Kitzing YX, Prando A, Varol C, Karczmar GS, Maclean F, Oto A. Benign conditions that mimic prostate carcinoma: MR imaging features with histopathologic correlation. *Radiographics* 2016;36(01):162–175
- 26 Gatti M, Faletti R, Gentile F, et al. mEPE-score: a comprehensive grading system for predicting pathologic extraprostatic extension of prostate cancer at multiparametric magnetic resonance imaging. *Eur Radiol* 2022;32(07):4942–4953
- 27 Roethke M, Kaufmann S, Knies M, et al. Seminal vesicle invasion: accuracy and analysis of infiltration patterns with high-spatial resolution T2-weighted sequences on endorectal magnetic resonance imaging. *Urol Int* 2014;92(03):294–299
- 28 Masterson TA, Pettus JA, Middleton RG, Stephenson RA. Isolated seminal vesicle invasion imparts better outcomes after radical retropubic prostatectomy for clinically localized prostate cancer: prognostic stratification of pt3b disease by nodal and margin status. *Urology* 2005;66(01):152–155
- 29 Hull GW, Rabbani F, Abbas F, Wheeler TM, Kattan MW, Scardino PT. Cancer control with radical prostatectomy alone in 1,000 consecutive patients. *J Urol* 2002;167(2 Pt 1):528–534
- 30 Ramsden AR, Chodak G. An analysis of risk factors for biochemical progression in patients with seminal vesicle invasion: validation of Kattan's nomogram in a pathological subgroup. *BJU Int* 2004;93(07):961–964
- 31 Ohori M, Scardino PT, Lapin SL, Seale-Hawkins C, Link J, Wheeler TM. The mechanisms and prognostic significance of seminal vesicle involvement by prostate cancer. *Am J Surg Pathol* 1993;17(12):1252–1261
- 32 Osborn JR, Ramsden AR, Chodak GW, Persad RA. Should the therapeutic approach to prostate cancer with seminal vesicle invasion be reviewed: improving functional results without diminishing oncological outcome? *BJU Int* 2004;94(04):482–483
- 33 Wang L, Hricak H, Kattan MW, Chen HN, Scardino PT, Kuroiwa K. Prediction of organ-confined prostate cancer: incremental value of MR imaging and MR spectroscopic imaging to staging nomograms. *Radiology* 2006;238(02):597–603
- 34 Djavan B, Zlotta A, Kratzik C, et al. PSA, PSA density, PSA density of transition zone, free/total PSA ratio, and PSA velocity for early detection of prostate cancer in men with serum PSA 2.5 to 4.0 ng/mL. *Urology* 1999;54(03):517–522
- 35 Nordström T, Akre O, Aly M, Grönberg H, Eklund M. Prostate-specific antigen (PSA) density in the diagnostic algorithm of prostate cancer. *Prostate Cancer Prostatic Dis* 2018;21(01):57–63